COMMENTARY

MRI monitoring of energy storage in vivo using magnetization pathways

Elena Vinogradov[a,b,1]

Primary storage of energy in mammalian tissue is glycogen, a branched polysaccharide form of glucose. Glycogen serves a central role in glucose homeostasis and is crucial for proper system functioning. Altered glycogen metabolism is manifested in a variety of disorders such as diabetes, liver diseases, glycogen storage diseases, and cancer. Currently, invasive biopsy remains the typical method for glycogen monitoring, since there is no accepted noninvasive method. Noninvasive methods to monitor and quantify glycogen in vivo would be of tremendous advantage and would provide key information on the range of diseases.

Such methods have been proposed, utilizing positron emission tomography (1), ultrasound (2), and magnetic resonance (MR) spectroscopy (3, 4). The imaging methods, if successful, would offer the advantage of spatial assessment of glycogen distribution noninvasively. However, at present, none of the proposed methods has proven to be robust, reliable, or practical for routine use and translation to clinical practice. In PNAS, Zhou et al. (5) introduce an MRI method for glycogen mapping relying only on endogenous molecules and manipulation of their magnetization via radiofrequency (RF) pulses. The approach has the potential to overcome limitations of previous technologies and become a game changer for the noninvasive mapping of glycogen in vivo.

The proposed method employs the so-called nuclear Overhauser effect (NOE) to achieve MRI contrast. NOE is part of the family of magnetization transfer (MT) methods for MR molecular imaging conb trast generation. Typically, only relatively mobile molecules and molecules with protons present at high concentration, like water, are visible on MRI ("water pool"). However, there are molecules, macromolecules, and molecular structures that are not visible, either due to low concentration or short transverse (T_2) relaxation times ("invisible pool"). They possess distinct chemical shifts and/or are present in a different magnetic environment from each other and water. They can be magnetically coupled to each other and/or to water. In the most general terms, this coupling could be due to two mechanisms as schematically depicted in Fig. 1: 1) through-space dipolar-induced cross-relaxation, or 2) chemical rearrangement (exchange). The dipolar-induced effect does not involve physical movement between two different magnetic environments, while chemical rearrangement does. All of the MT methods discussed here employ RF pulses to saturate (i.e., destroy) magnetization in one pool and observation of the decrease in magnetization in another, magnetically coupled pool. The MT effect can involve direct transfer between two pools or can consist of multiple transfer pathways, involving both mechanisms (Fig. 1). The MT contrast due to the presence and integrity of semisolid structures (with short T_2) had been explored since the early 1990s and had reached clinical practice [MT contrast (6)]. In addition, there are many moieties that have long T_2 values but are not MRI visible due to their low concentration. In MRI applications, the MT involving dipolar-induced relaxation pathways from these mobile moieties is referred to as the NOE (7, 8) (more precisely relayed NOE), while that involving pure chemical rearrangement has been called chemical exchange saturation transfer (CEST) (9, 10). The advantage of these MT methods is that they generate a contrast that leads to information on the microstructural and molecular level, distinctive from the standard T_1 and T_2 differences. They offer a way to explore endogenous molecules, without the need for injections of exogenous substances.

CEST has gained significant interest lately (11–13). Due to the nature of the process, it is sensitive to important tissue markers, like pH or temperature, and can serve as a metabolite sensor. CEST using amide groups in protein side chains [amide proton transfer (14)] has been gaining recognition as a tumor monitoring method, especially in neuro applications (11–13, 15). Recent preclinical and clinical studies had applied CEST to monitor brain, prostate, and breast

[a]Department of Radiology, University of Texas Southwestern Medical Center, Dallas, TX 75390; and [b]Advanced Imaging Research Center, University of Texas Southwestern Medical Center, Dallas, TX 75390

Author contributions: E.V. wrote the paper.

The author declares no competing interest.

See companion article, "Magnetic resonance imaging of glycogen using its magnetic coupling with water," 10.1073/pnas.1909921117.

[1]Email: elena.vinogradov@utsouthwestern.edu.

First published February 28, 2020.

www.pnas.org/cgi/doi/10.1073/pnas.2001048117

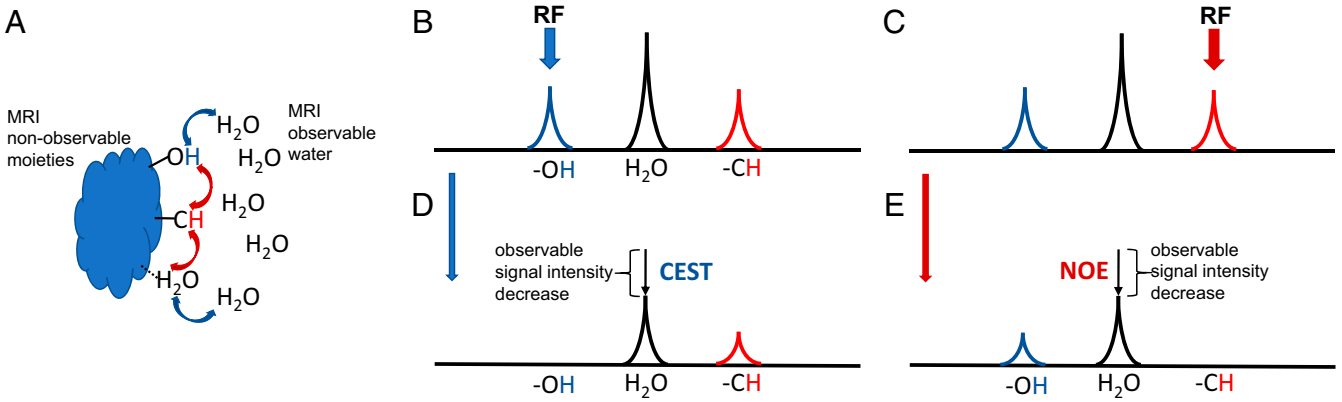

Fig. 1. Schematic of MT pathways and select MT experiments. (*A*) Protons are coupled by 1) dipolar induced cross-relaxation (red arrows), a through-space MT mechanism that does not involve physical rearrangement; or 2) chemical rearrangement (blue arrows) involving physical motion of protons. MRI-invisible moieties are surrounded by water (MRI observable). (*B* and *C*) Schematic of proton NMR spectrum (not to scale) showing spectral lines of chemically exchanging group (e.g., –OH), water, and dipolar cross-relaxation coupled group (e.g., –CH). RF saturation is applied either at –OH resonance (blue arrow) leading to CEST effect (*D*) or at –CH resonance (red arrow) leading to NOE effect (*E*). While only –OH and –CH groups are shown here for the sake of simplicity, other exchanging or coupled protons can be used. Only the basic of possible pathways are depicted.

tumors and had indicated correlation of CEST with cancer aggressiveness markers, such as grade, proliferation index Ki-67, or ER/PR/HER2 status (11–13, 15). CEST had also been explored as a metabolite marker. Examples include, but are not limited to, glutamate, creatine, glycosaminoglycans, and myo-inositol (11–13, 15).

Previously, van Zijl et al. (16) had applied CEST to detect glycogen in perfused liver. This work utilized hydroxyl protons in glycogen, resonating at +1 ppm from water (glycoCEST). The potential advantages of glycoCEST include utilization of endogenous glycogen, no need for specialized MRI hardware, and the ability to generate high-resolution images. However, with the exception of a couple of studies (17), the method had not been applied in vivo. This is due to combination of several factors, such as fast exchange of hydroxyl protons, the proximity of their chemical shift to the water resonance, and potential overlap with other molecules. For example, glycoCEST is sensitive to any exchanging protons resonating at +1 ppm from water; thus, free glucose is also detected in addition to glycogen. All of these factors render the method to be highly challenging in vivo and at clinically relevant field strengths (3 T).

While contrast using CEST had been actively explored, by comparison contrast involving NOE was largely overlooked. It is more challenging to identify and typically require higher fields (≥7 T) to observe clearly. To the best of our knowledge, the first observation of the NOE effect in MRI setting was in cartilage, by Ling et al. (8). Following this, NOE contrast has been explored in various studies at high field (18). A potential advantage of NOE over CEST is that it is generally weaker to nonexistent dependence on pH, making potential quantification easier. The potential limitation of NOE, however, is that at present it has only been reported in the studies at high field, thus limiting its exploration to animal studies (where high-field MRIs are more prevalent) and to a few centers with human, 7-T or higher MRI systems.

In PNAS, Zhou et al. (5) use the NOE mechanism to create MRI contrast weighted by glycogen. The method is dubbed glycoNOE. Here, the aliphatic protons appearing as a broad peak at approximately −1 ppm from water are saturated. There are at least two potential pathways for saturation to go from here to reach observable water (as is depicted in figure 1 of their paper): 1) to hydroxyl proton via direct NOE followed by chemical exchange with water, and 2) to proximal bound water, which becomes dynamically free. This is in contrast to the previous glycoCEST method, which generally involved saturation of hydroxyl protons and "direct" transfer via chemical rearrangement. In addition, the NOE effect is generated from larger molecules with relatively slow motion. Thus, glycoNOE can be generated from glycogen, but not from free glucose, making the method more specific.

Interestingly and importantly, Zhou et al. observed a linear dependence of glycoNOE on glycogen concentration in vitro. While further validation and potential calibration of the effects is needed, this may open the door for quantification of glycoNOE and generation of glycogen concentration maps noninvasively at high spatial resolution. At the same time, they observed the dependence of the glycoNOE effect on the size of the glycogen particles. Different glycogen particle sizes coexist in liver (between 10 and 300 nm), which may complicate the quantification of the results in the future. It should be noted that the dependence of glycoNOE on the particle size is in agreement with the nature of this contrast. The NOE effect is motion dependent, and slower motion of larger particles may lead to stronger NOE effects. Importantly, glycoNOE in liver was markedly decreased after fasting and following glucagon infusion. This is a good demonstration of potential of the method for future application in metabolic studies.

The biggest impact of glycoNOE would be a successful translation to human MRI studies. The authors make an important step toward this by demonstrating (in SI Appendix of ref. 5) in vitro results at the clinically relevant field strength of 3 T. This is the second most prevalent field strength in clinical use today, surpassed only by even lower 1.5 T. Transition to lower field inevitably brings spectral lines closer together in absolute hertz values, which may lead to artifacts due to peak coalescences and increased direct water saturation. While the basic physics remains the same as in test tubes, measurements in humans will be complicated by motion, large static field distributions, blood flow, etc. Special care must be taken with influence of lipid (fat) signal on glycoNOE. Endogenous fat is a known source of artifacts in body MRI imaging. Moreover, many tumors exhibit abnormal lipid metabolism. These lipids are not participating in MT, but their magnetization might be affected by saturation pulses and will be present in the observed signal, due to partial volume effects, leading to contamination of glycoNOE contrast. Thus, efficient

removal of non-MT participating fat signal is paramount. This could be achieved effectively with methods like Dixon approach (19), which do not require additional saturation and were combined with CEST previously (20).

In summary, glycoNOE (5) offers a path toward the noninvasive mapping of glycogen. The approach does not require injections or additional hardware and only requires software modifications comparable to a software upgrade. Taken together with the prevalence of glycogen in tissues and its importance in a host of diseases, glycoNOE may open a door to exciting opportunities for basic and clinical MR molecular-imaging applications.

Acknowledgments

I would like to thank Dr. Lenkinski for the helpful discussions and feedback on the manuscript. This research is supported in part by Cancer Prevention and Research Institute of Texas Grant RP180031.

1 T. H. Witney *et al.*, A novel radiotracer to image glycogen metabolism in tumors by positron emission tomography. *Cancer Res.* **74**, 1319–1328 (2014).
2 D. C. Nieman, R. A. Shanely, K. A. Zwetsloot, M. P. Meaney, G. E. Farris, Ultrasonic assessment of exercise-induced change in skeletal muscle glycogen content. *BMC Sports Sci. Med. Rehabil.* **7**, 9 (2015).
3 P. A. Bottomley, C. J. Hardy, P. B. Roemer, O. M. Mueller, Proton-decoupled, Overhauser-enhanced, spatially localized carbon-13 spectroscopy in humans. *Magn. Reson. Med.* **12**, 348–363 (1989).
4 R. Ouwerkerk, R. I. Pettigrew, A. M. Gharib, Liver metabolite concentrations measured with ^{1}H MR spectroscopy. *Radiology* **265**, 565–575 (2012).
5 Y. Zhou *et al.*, Magnetic resonance imaging of glycogen using its magnetic coupling with water. *Proc. Natl. Acad. Sci. U.S.A.* **117**, 3144–3149 (2020).
6 S. D. Wolff, R. S. Balaban, Magnetization transfer contrast (MTC) and tissue water proton relaxation in vivo. *Magn. Reson. Med.* **10**, 135–144 (1989).
7 A. W. Overhauser, Polarization of nuclei in metals. *Phys. Rev.* **92**, 411–415 (1953).
8 W. Ling, R. R. Regatte, G. Navon, A. Jerschow, Assessment of glycosaminoglycan concentration in vivo by chemical exchange-dependent saturation transfer (gagCEST). *Proc. Natl. Acad. Sci. U.S.A.* **105**, 2266–2270 (2008).
9 K. M. Ward, A. H. Aletras, R. S. Balaban, A new class of contrast agents for MRI based on proton chemical exchange dependent saturation transfer (CEST). *J. Magn. Reson.* **143**, 79–87 (2000).
10 K. M. Ward, R. S. Balaban, Determination of pH using water protons and chemical exchange dependent saturation transfer (CEST). *Magn. Reson. Med.* **44**, 799–802 (2000).
11 P. C. M. van Zijl, N. N. Yadav, Chemical exchange saturation transfer (CEST): What is in a name and what isn't? *Magn. Reson. Med.* **65**, 927–948 (2011).
12 E. Vinogradov, A. D. Sherry, R. E. Lenkinski, CEST: From basic principles to applications, challenges and opportunities. *J. Magn. Reson.* **229**, 155–172 (2013).
13 K. M. Jones, A. C. Pollard, M. D. Pagel, Clinical applications of chemical exchange saturation transfer (CEST) MRI. *J. Magn. Reson. Imaging* **47**, 11–27 (2018).
14 J. Zhou, J.-F. Payen, D. A. Wilson, R. J. Traystman, P. C. M. van Zijl, Using the amide proton signals of intracellular proteins and peptides to detect pH effects in MRI. *Nat. Med.* **9**, 1085–1090 (2003).
15 B. K. H. Law *et al.*, Head and neck tumors: Amide proton transfer MRI. *Radiology* **288**, 782–790 (2018).
16 P. C. M. van Zijl, C. K. Jones, J. Ren, C. R. Malloy, A. D. Sherry, MRI detection of glycogen in vivo by using chemical exchange saturation transfer imaging (glycoCEST). *Proc. Natl. Acad. Sci. U.S.A.* **104**, 4359–4364 (2007).
17 M. Deng *et al.*, Chemical exchange saturation transfer (CEST) MR technique for liver imaging at 3.0 tesla: An evaluation of different offset number and an after-meal and over-night-fast comparison. *Mol. Imaging Biol.* **18**, 274–282 (2016).
18 M. Zaiss *et al.*, Downfield-NOE-suppressed amide-CEST-MRI at 7 Tesla provides a unique contrast in human glioblastoma. *Magn. Reson. Med.* **77**, 196–208 (2017).
19 W. T. Dixon, Simple proton spectroscopic imaging. *Radiology* **153**, 189–194 (1984).
20 S. Zhang *et al.*, CEST-Dixon for human breast lesion characterization at 3 T: A preliminary study. *Magn. Reson. Med.* **80**, 895–903 (2018).